Upconversion processes in Pr^{3+}-doped chalcohalide glasses

2001 J. Phys.: Condens. Matter 13 10347

(http://iopscience.iop.org/0953-8984/13/46/307)

INSTITUTE OF PHYSICS PUBLISHING JOURNAL OF PHYSICS: CONDENSED MATTER

J. Phys.: Condens. Matter **13** (2001) 10347–10358 PII: S0953-8984(01)25704-X

Upconversion processes in Pr^{3+}-doped chalcohalide glasses

J Fernández[1,2,3], R Balda[1,2,3], A Mendioroz[1] and A J García-Adeva[4]

[1] Departamento de Física Aplicada I, ETSII y Telecomunicación Alameda Urquijo s/n 48013, Bilbao, Spain
[2] Centro Mixto CSIC/UPV/EHU, ETSII y Telecomunicación Alameda Urquijo s/n 48013, Bilbao, Spain
[3] DIPC, ETSII y Telecomunicación Alameda Urquijo s/n 48013, Bilbao, Spain
[4] Department of Physics, University of Wisconsin, Madison, WI-53706, USA

Received 12 June 2001
Published 2 November 2001
Online at stacks.iop.org/JPhysCM/13/10347

Abstract

Infrared-to-visible upconversion obtained under continuous-wave infrared laser excitation has been investigated in Pr^{3+}-doped chalcohalide glasses for different halide (Cl, Br, I) modifiers and Pr^{3+} concentrations. The excitation wavelength dependence suggests two different upconversion mechanisms. When the excitation wavelength is resonant with the $^1G_4$ state an orange fluorescence from the $^1D_2$ state is observed which is attributed to energy-transfer upconversion, whereas nonresonant excitation at higher energies than the $^1G_4$ level originates emission from the $^3P_0$ state. This latter upconverted emission can be attributed to excited-state anti-Stokes absorption assisted by phonon emission. A model accounting for the photon–ion–phonon interaction is in good agreement with the observed temperature dependence of the excitation-upconverted fluorescence band. Orange-to-blue upconversion has also been observed and analysed for all the samples.

1. Introduction

With the development of high-capacity telecommunication networks, research has been directed at finding new rare-earth-doped glasses for optical fibre amplifiers. Glasses with phonon energies lower than those of silica can display more efficient amplification, which results in devices that can operate at wavelengths not accessible with silica. These include, for example, praseodymium-doped fluoride or sulphide glass optical amplifiers [1, 2].

On the other hand, low-phonon-energy glasses have also been investigated as potential materials for efficient upconversion of infrared (IR) into visible (VIS) light [3]. Sulphide glasses, however, usually show a low-energy band gap that causes strong absorption of visible light, as in Ga- and Ge-based glasses [4, 5]. This drawback is partly circumvented in Ge–Ga–S ternary glasses (GGS) by incorporating a caesium halide. Thus, addition of chlorine,

bromine, or iodine ions results in a decrease of sulphur concentration within the glass and a consequent shift of the visible transparency towards shorter wavelengths. In addition, large cations such as caesium act as network modifiers and open the tetrahedral structure of GGS glass. Therefore, the degree of disorder is higher in the GGS–CsX (X = Cl, Br, I) system, and more stable glasses are formed compared to GGS [6]. It is found that CsX can be introduced with no significant reduction of the infrared transparency and rare-earth solubility of these chalcohalide glasses. Moreover, rare-earth-doped chalcohalide glasses are expected to show high radiative efficiencies because their phonon energies are lower than in fluoride glasses, which reduces nonradiative losses due to multiphonon relaxation.

Trivalent praseodymium is an attractive optical activator which offers the possibility of simultaneous blue, green, and red emission for laser action, as well as IR emission for optical amplification at 1.3 μm [7]. Pr^{3+} systems are also interesting as short-wavelength upconversion laser materials [8, 9]. Frequency upconversion processes have received increasing attention in recent years as a mechanism for producing new laser transitions. From a fundamental point of view, the study of frequency upconversion processes is also important for understanding the mechanisms of interaction between the rare-earth (RE) ions in different hosts [10]. As a consequence, several investigations have been undertaken in an effort to understand the dynamics of the IR-to-VIS upconversion in crystals as well as in bulk glass and glass fibres. The blue anti-Stokes fluorescence resulting from the $^3P_0 \rightarrow {}^3H_4$ transition generated by pumping the $^1D_2$ state has been extensively studied [11–20]. However, until very recently, IR-to-orange (the $^1G_4 \rightarrow {}^1D_2$ process) and IR-to-blue (the $^1G_4 \rightarrow {}^3P_0$ process) upconversion processes have only been observed in a few cases [21–23] in single-Pr^{3+}-doped systems. These processes are important not only for obtaining visible emission pumping by using infrared sources, but also because they can impair the performance of optical amplifiers operating at 1.3 μm.

In a previous work the authors characterized the visible luminescence of the Pr^{3+} ion in halide modified sulphide glasses; this work included a preliminary study of the visible emission spectra obtained under continuous-wave (cw) infrared excitation in the $^1G_4$ state [24]. The analysis of the upconverted fluorescence as a function of the excitation wavelength indicated the existence of two different upconversion mechanisms (anti-Stokes absorption (ESA) and energy-transfer upconversion (ETU)) populating the $^3P_0$ and the $^1D_2$ levels respectively.

In this work we report a detailed analysis of the infrared-to-blue and infrared-to-orange luminescence associated with the $^1G_4$ state together with the blue upconversion obtained by pumping the $^1D_2$ level.

Relating to the $^1G_4$ level, two different mechanisms have been identified in the two-photon processes involved in the upconversion luminescence. The blue emission is associated with a sequential two-photon absorption in which the Pr^{3+} ion in its ground state absorbs a photon nonresonantly and ends up in the $^1G_4$ excited state, assisted by a phonon emission. Then a second IR photon is resonantly absorbed and the ^3P_J, $^1I_6$ multiplets are reached. The temperature dependence of the excitation spectrum of the blue upconverted emission has been modelled, on the basis of the photon–ion–phonon interaction process. The model prediction gives a good agreement with the experimental results. The second mechanism giving rise to the orange emission is a typical energy-transfer upconversion process. As far as we know, this is the first time that both kinds of process have been seen to coexist in the same excited level and have been simultaneously measured in a single-Pr^{3+}-doped bulk glass. Moreover, we show that it is possible to select one of them by continuous excitation wavelength tuning.

On the other hand, the rise time shown by the blue emission obtained under pulsed excitation in the $^1D_2$ level suggests that energy-transfer processes are mainly responsible for the upconverted emission.

2. Experimental procedure

The glasses used in this work were prepared at the Laboratoire des Verres et Céramiques of the University of Rennes (France). The composition $50GeS_2$–$25Ga_2S_3$–25CsX where X is Cl, Br, or I was found to give the most thermally stable glasses. These glasses are coded GGSC, GGSB, and GGSI, respectively.

The chalcohalide glasses were prepared from elemental starting products and salts, which were measured and weighed in a low-humidity argon-atmosphere glove box. This precaution minimized the risk of contamination by oxygen and water impurities. 5N high-purity germanium and gallium ingots and sulphur chips along with 3N-purity caesium halides were batched into a silica ampoule. Praseodymium was added as $PrCl_3$. The ampoule was then pumped under vacuum to 10^{-4} Torr for several hours and sealed by using an oxyacetylene torch.

Once sealed, the ampoule was protected with a grille and placed in a tubular oven equipped with a rocking apparatus. Samples were heated to the reaction temperature at a very slow rate, typically 3 °C per minute, to avoid explosion due to unreacted sulphur gas phases. Halide-modified glass compositions were found to react more quickly than pure sulphide compounds which usually require low heating rates of about 1 °C min^{-1}.

Once the reaction temperature was reached, rocking for at least six hours mixed the constituents. The reaction temperature for all glasses was 925 °C. The temperature of the synthesis oven was then reduced and the oven was held in a vertical position while rocking stopped. For the highest-optical-quality glasses, the compositions were maintained for several hours at the lowest possible temperature without crystallization, typically 700 °C. This allowed the glass to settle, minimizing bubbles and composition micro-inhomogeneities. The glasses were then quenched in air for about 30 seconds and then transferred to the annealing oven, which was held at the glass transition temperature. It should be noted that the slowest possible quenching rate with no crystallization usually results in the best-quality glasses.

The samples were cut and polished into discs or cubes, with their thickness varying from 1.0 cm to 0.5 mm, to be used in transmission spectroscopy and upconversion measurements. The samples were doped with 0.5% of Pr^{3+}. The glass GGSB was doped with 0.2, 0.5, and 0.7 mol% of Pr^{3+}.

The samples temperature was varied between 4.2 and 300 K with a continuous-flow cryostat. The emission measurements were made by using a Ti–sapphire ring laser (0.4 cm^{-1} linewidth) in the 900–1060 nm range. The fluorescence was analysed with a 0.25 m monochromator, and the signal was detected by a Hamamatsu R928 photomultiplier and finally amplified by a standard lock-in technique.

Lifetime measurements and orange-to-blue upconversion studies were carried out by exciting the samples with a tunable dye laser, pumped by a pulsed frequency-doubled Nd:YAG laser (9 ns pulse width), and detecting the emission with a Hamamatsu R928 photomultiplier. Data were processed by an EGG-PAR boxcar integrator.

3. Results and discussion

3.1. IR-to-VIS upconversion

Figure 1 shows the room temperature emission spectra for GGSB glass doped with 0.2% of Pr^{3+} ions obtained by exciting the $^1G_4$ state resonantly and nonresonantly. This figure also includes the emission spectrum obtained under one-photon (OP) excitation in the $^3P_2$ level for comparison (figure 1(a)). Figure 1(b) shows the room temperature spectrum for GGSB glass obtained by resonantly exciting the $^1G_4$ state (1020 nm). As can be observed, the main

emission corresponds to the $^1D_2$ state with a weak emission from the $^3P_0$ level at 500 nm and 654 nm. However, if excitation is performed nonresonantly at higher energies (979 nm), the spectrum (figure 1(c)) is similar to the one obtained under OP visible excitation. In this case the main emission corresponds to the $^3P_0$ and $^3P_1$ levels as identified in the direct emission spectrum by exciting at 454 nm. To illustrate the IR excitation wavelength dependence of the visible upconverted emission, figure 2 shows the emission spectra obtained under different IR excitation wavelengths for GGSC glass at 77 K. As can be observed, at high energies when the excitation wavelength is not resonant with the $^3H_4 \rightarrow {}^1G_4$ transition, the spectrum is similar to the one obtained under direct OP excitation in the $^3P_2$ level. It can be noticed that since thermalization is decreased at 77 K, the emissions from the level $^3P_1$, observable in the room temperature emission spectra, are extinguished. As the excitation wavelength increases, the relative intensities of the emission from the level $^3P_0$ and that from $^1D_2$ change. The emission from the state $^1D_2$ increases whereas that from the level $^3P_0$ decreases, and finally near the resonance with the $^3H_4 \rightarrow {}^1G_4$ transition, the emission corresponds mainly to the orange $^1D_2 \rightarrow {}^3H_4$ transition. The same behaviour was found in all three glasses.

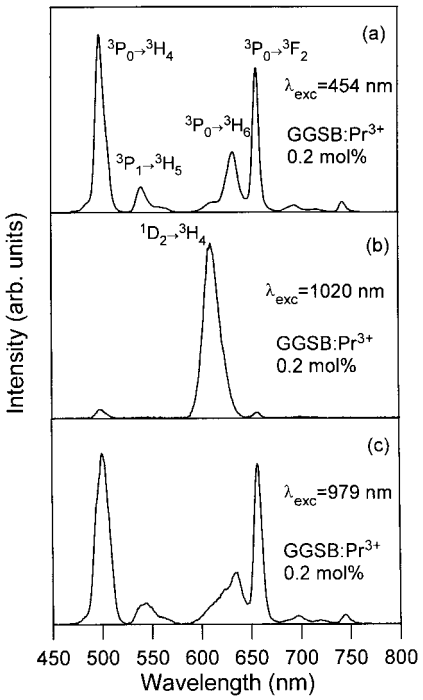

Figure 1. Room temperature emission spectra obtained (a) under excitation at 454 nm, and (b) and (c) under IR excitation for GGSB glass doped with 0.2% of Pr^{3+}.

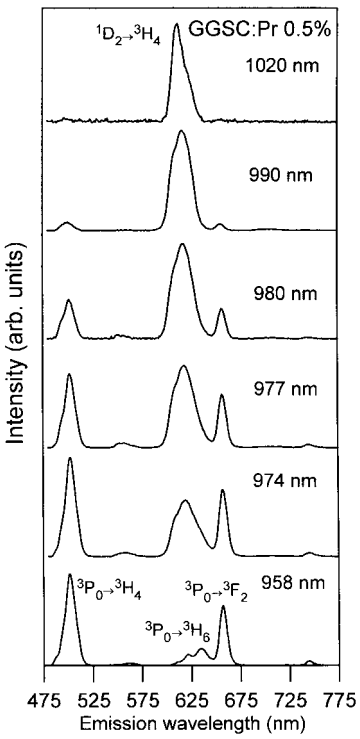

Figure 2. Steady-state emission spectra obtained at different IR excitation wavelengths for the glass GGSC doped with 0.5% of Pr^{3+}. The data correspond to 77 K.

The upconverted fluorescence from the level $^1D_2$ obtained under resonant excitation of the state $^1G_4$ shows a close quadratic dependence on the pumping power for all samples, which indicates a two-photon (TP) process. This in turn may be associated with excited-state absorption (ESA) and/or to energy-transfer upconversion (ETU) [25, 26]. The same behaviour is observed for the blue emission from the level $^3P_0$ obtained under nonresonant excitation. The same occurs for all samples. Figure 3 shows a logarithmic plot of the integrated emission

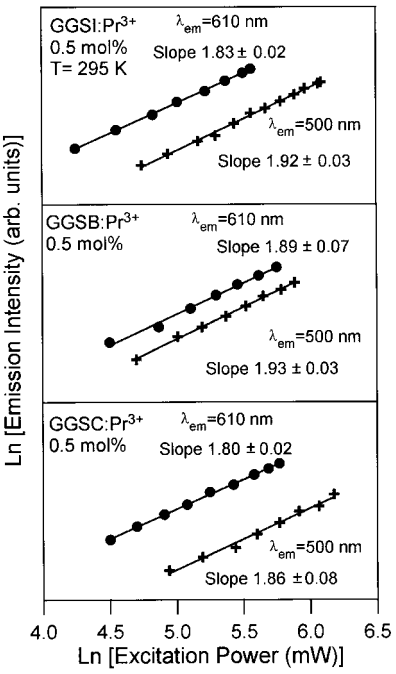

Figure 3. Logarithmic plots of the integrated intensities of the upconverted emission from $^3P_0$ (500 nm) and $^1D_2$ (610 nm) levels obtained under nonresonant and resonant IR excitation, respectively, for the three glasses doped with 0.5% of Pr^{3+}.

intensities of the upconverted fluorescence as a function of the pumping power for the three glasses doped with 0.5% of Pr^{3+}.

Excitation spectra of the upconverted emission from states $^3P_0$ and $^1D_2$ at 500 nm and 610 nm respectively were taken at different temperatures between 4.2 K and 295 K. As can be seen in figure 4, the excitation spectrum of the fluorescence from the $^1D_2$ state shows the same features as the $^3H_4 \rightarrow {}^1G_4$ absorption spectrum. This behaviour indicates that an ETU process seems to be responsible for the observed luminescence. On the other hand, the excitation spectrum corresponding to the blue emission from the level $^3P_0$ shows a broad band centred around 960 nm. It is worth mentioning that the energy corresponding to the

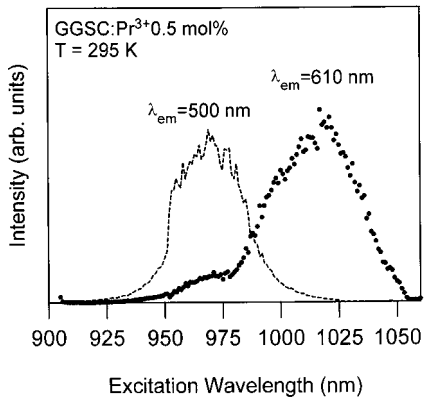

Figure 4. Excitation spectra of the upconverted emission from $^3P_0$ (500 nm) and $^1D_2$ levels (610 nm) for GGSC glass doped with 0.5% of Pr^{3+} obtained at room temperature.

barycentre of this band added to the energy of the level $^1G_4$ agrees with the $^3H_4 \rightarrow {}^3P_0$ transition energy. The temperature dependences of the excitation spectra are also different for the two emissions: whereas the emission from the level $^1D_2$ (obtained under resonant excitation) is nearly independent of temperature, the emission from the level $^3P_0$ (obtained under nonresonant excitation) increases with temperature which suggests that we are dealing with a phonon-assisted process.

All the results presented above lead us to infer the existence of two different mechanisms for populating both $^3P_0$ and $^1D_2$ states under cw IR excitation. The origins of the two mechanisms are discussed below.

3.1.1. The $^1D_2$ level. As we have seen, the upconverted orange fluorescence from the $^1D_2$ level, obtained under resonant excitation of the $^1G_4$ level, shows a clear quadratic dependence on pumping power and is independent of temperature for all glasses. This level can be populated by ETU involving the $^1G_4$ level ($^1G_4$, $^1G_4$) $\rightarrow$ ($^1D_2$, $^3H_5$) and by ESA involving Pr^{3+} ions in the intermediate $^3F_4$ level. In the latter case, the $^3F_4$ level must be sufficiently populated. This may arise through either of two different processes: (i) multiphonon relaxation or (ii) cross relaxation of the $^1G_4 \rightarrow {}^3H_5$ and $^3H_4 \rightarrow {}^3F_4$ transitions. Multiphonon relaxation is unlikely to occur in these glasses due to the energy gap between $^1G_4$ and $^3F_4$ levels (3300 cm^{-1}) and the phonon energies involved (340 cm^{-1}). Spectroscopic data reveal that cross relaxation of the $^1G_4$ level via $^1G_4 \rightarrow {}^3H_5$ and $^3H_4 \rightarrow {}^3F_4$ transitions has an energy mismatch of around 650 cm^{-1} and should be temperature dependent. However, in the preceding paragraph we have seen that the upconverted emission from the $^1D_2$ level is independent of temperature. In conclusion, the experimental results together with the energy level diagram shown in figure 5 suggest that a possible explanation for the population of the $^1D_2$ level could be an ETU process involving the $^1G_4$ level ($^1G_4$, $^1G_4$) $\rightarrow$ ($^1D_2$, $^3H_5$). In such a process two ions in the $^1G_4$ state interact and one ion loses energy and goes to the $^3H_5$ state, whereas the other one gains energy and goes to the $^1D_2$ state from where orange emission occurs.

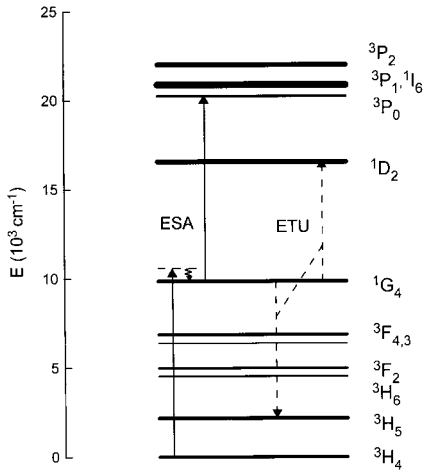

Figure 5. The energy level diagram of Pr^{3+} in GGSB glass obtained from the low-temperature (10 K) absorption spectrum. Possible upconversion mechanisms for populating the $^3P_0$ and $^1D_2$ levels under nonresonant and resonant excitation of the $^1G_4$ state are also indicated.

3.1.2. The $^3P_0$ level. As we mentioned above, after nonresonant excitation of the $^1G_4$ level, we observed upconversion from the level $^3P_0$ in all samples studied. This emission shows a quadratic dependence on the pumping power and increases with temperature from 4.2 K to 295 K.

According to the energy level scheme in figure 5, obtained from the low-temperature absorption spectrum for GGSB glass, an ESA absorption seems to be the mechanism most likely to populate the $^3P_0$ level. In this process a Pr^{3+} ion in its ground state absorbs a photon nonresonantly and ends up in the $^1G_4$ excited state, assisted by a phonon emission. Then a second IR photon is resonantly absorbed and the $^3P_0$ state is reached. This type of upconversion process has also been shown to occur in fluoride glasses and crystals [21–23].

When resonantly pumping the $^1G_4$ level, there is not enough energy to excite the $^3P_0$ level by a sequential TP process. However, the emission spectra at room temperature show that some weak emissions of the $^3P_0$ level exist for this pumping energy. Emissions from the $^3P_0$ level at this energy cannot be attributed to the above-mentioned two-photon process. In this case the $^3P_0$ population roughly behaves as the third power (2.6) of the cw laser excitation, which implies either ETU processes involving three ions or stepwise absorption of three photons via nonresonant absorption [22].

3.1.3. A model for upconversion emission from the $^3P_0$ level. As stated above, the most likely explanation for the upconversion emission from the $^3P_0$ level is an ESA process. Therefore, it is interesting to study whether the temperature dependence of the calculated integrated intensity for this kind of process is in agreement with the observed one.

Therefore, let us consider a Hamiltonian model in which an impurity ion interacts with both the laser field and the phonons in the solid [27, 28].

The probability per unit time of a process in which the Pr^{3+} ion in its ground state absorbs an incident photon, a phonon is created or annihilated, and the ion goes up to the excited state is easily evaluated as a second-order process in perturbation theory. Details of the calculation can be found in references [27] and [29], and will not be presented here.

The final expression for the probability of such a process is found to be

$$w = \pi \frac{(\hat{e}_L \cdot \boldsymbol{\mu})^2 \Lambda^2 n}{2\varepsilon_0 V \rho v^2} \frac{\omega_0^2}{\omega_L} \frac{P(\hbar\omega_0 - \hbar\omega_L) f(\hbar\omega_0 - \hbar\omega_L)}{\hbar\omega_0 - \hbar\omega_L} \qquad \text{if } \hbar\omega_0 > \hbar\omega_L \tag{1a}$$

and

$$w = \pi \frac{(\hat{e}_L \cdot \boldsymbol{\mu})^2 \Lambda^2 n}{2\varepsilon_0 V \rho v^2} \frac{\omega_0^2}{\omega_L} \frac{P(\hbar\omega_L - \hbar\omega_0) [f(\hbar\omega_L - \hbar\omega_0) + 1]}{\hbar\omega_L - \hbar\omega_0} \qquad \text{if } \hbar\omega_0 < \hbar\omega_L. \tag{1b}$$

In these expressions, n is the photon density of the incident beam, f is the Bose–Einstein function, and P is the phonon density of states. Expression (1a) corresponds to the Stokes part leading to a cooling process [29], whereas expression (1b) stands for the anti-Stokes counterpart of this process, namely, anti-Stokes warming.

Let us now turn our attention to the phonon density of states appearing in (1). Raman measurements performed on these glasses showed an asymmetric, Gaussian-like, broad band centred around 340 cm^{-1} which corresponds to a breathing mode of the GeS_4 and GaS_4 groups [30, 31]. Therefore, a Gaussian-like function was selected as a plausible function for the phonon density of states. In order to avoid a divergence in the transition probability at the resonance $\hbar\omega_0 = \hbar\omega_L$, the Gaussian function was scaled by the Debye distribution function in such a way that at low phonon energies the distribution function resembles the Debye one, whereas it is close to a Gaussian at the centre of the distribution. This choice avoids the introduction of a cut-off at low phonon frequencies, and therefore the introduction of unnecessary parameters

in the model, and qualitatively resembles the features found in Raman spectroscopy for the density of states of these modes. The form of the selected function is

$$P(E) = CE^2 \exp\left[-\left(\frac{E-\bar{E}}{\Gamma}\right)^2\right] \tag{2}$$

where E is the phonon energy, $\bar{E} = \hbar\bar{\omega}$ is the energy at the centre of the distribution, Γ its width, and C an adequate normalization constant.

In the case of chalcohalide glasses, on the basis of Raman measurements, the centre of the Gaussian function representing the phonon density of states was taken at 340 cm^{-1} and $\Gamma = 100\ \mathrm{cm}^{-1}$.

With this distribution function, expression (1) becomes

$$w = C\pi \frac{(\hat{\boldsymbol{e}}_L \cdot \boldsymbol{\mu})^2 \Lambda^2 n}{2\varepsilon_0 V \rho v^2} \frac{(\mp\hbar\omega_0 \pm \hbar\omega_L)\omega_0^2}{\omega_L} \times \exp\left[-\left(\frac{\mp\hbar\omega_0 \pm \hbar\omega_L - \hbar\bar{\omega}}{\Gamma}\right)^2\right] \begin{cases} f(\hbar\omega_L - \hbar\omega_0) + 1 \\ f(\hbar\omega_0 - \hbar\omega_L) \end{cases} \tag{3}$$

where the upper (lower) expression corresponds to the anti-Stokes (Stokes) part of warming (cooling).

The intensity of the upconverted fluorescence will be proportional to the population of the $^1\mathrm{G}_4$ excited-state level produced by these second-order processes and to the probability of ESA reabsorption to the high $^3\mathrm{P}_J$ multiplets. Therefore, if the emitting-level quantum efficiency is taken as one (as is estimated from the comparison between the experimental and calculated radiative lifetimes), the temperature dependence of the integrated fluorescence can be determined by comparing the experimental data with the expression

$$I(T) \sim \int w(\omega_L, T)\, \mathrm{d}\omega_L. \tag{4}$$

Substituting the anti-Stokes part of expression (3) in (4) gives

$$I(T) \sim \int_{\hbar\omega_0}^{\hbar\omega_0+\hbar\omega_D} \frac{\omega_L - \omega_0}{\omega_L} \exp\left[-\left(\frac{\omega_L - \omega_0 - \bar{\omega}}{\Delta\omega}\right)^2\right] [f(\omega_L - \omega_0) + 1]\ \mathrm{d}\omega_L \tag{5}$$

where $\hbar\bar{\omega} = \bar{E}$ and $\hbar\,\Delta\omega = \Gamma$. By introducing the variable $x = \omega_L - \omega_0$, we finally arrive at

$$I(T) \sim \int_0^{\omega_D} \frac{x}{\omega_0 + x} \exp\left[-\left(\frac{x-\bar{\omega}}{\Delta\omega}\right)^2\right] \frac{1}{1 - \exp(-x/k_B T)}\, \mathrm{d}x \tag{6}$$

where ω_D is the Debye frequency.

In order to compare the results of the numerical evaluation of the integrated intensity (expression (6)) with the experimental data, we have included the effect of inhomogeneous broadening by adding a constant temperature-independent background. Therefore

$$I(T) = a + b\Xi(T) \tag{7}$$

where Ξ is given by (6). Constants a and b contain averages over the inhomogeneous background (parameter a), or complicated combinations of the prefactors appearing in equation (3) (parameter b) and, therefore, their exact values are unimportant for our purposes.

Figure 6 shows the integrated intensity of the upconverted fluorescence of the excitation spectrum corresponding to the blue emission from the $^3\mathrm{P}_0$ level as a function of temperature. The continuous line is the fitting to the theoretical model given by equation (7). The only parameters used in this fitting are the constants in equation (7).

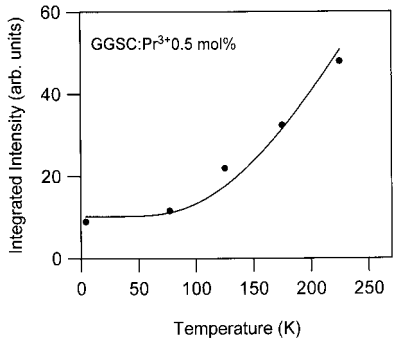

Figure 6. The integrated intensity of the upconverted fluorescence of the excitation spectra corresponding to the blue emission from the $^3P_0$ level as a function of temperature. Symbols correspond to the experimental data and solid line is the fitting to the theoretical model given by equation (7).

As can be seen, there is a good agreement between experimental results and the model prediction which gives support not only to the model hypothesis regarding the kind of process involved, but also to the distribution function used for the phonon energies. From a more fundamental point of view these results give us a guide to understanding why such upconversion processes are very sensitive to the particular distribution of phonon energies in the solid.

3.2. Orange-to-blue frequency upconversion

The existence of orange-to-blue upconverted fluorescence in this system has been investigated by directly exciting the $^1D_2$ level. We have observed anti-Stokes fluorescence from the $^3P_0 \rightarrow {}^3H_4$ transition in the 77 K–295 K temperature range for all samples and Pr^{3+} concentrations. Figure 7 shows the upconverted emission spectrum for GGSC glass doped with 0.5 mol% at 77 K obtained by exciting at 600 nm. The broad line is due to large site-to-site variations of the crystal-field strength. Similar spectra were obtained for the three glasses. For all samples the intensity of the anti-Stokes emission shows a quadratic dependence on the excitation laser energy, indicating that two photons participate in this process.

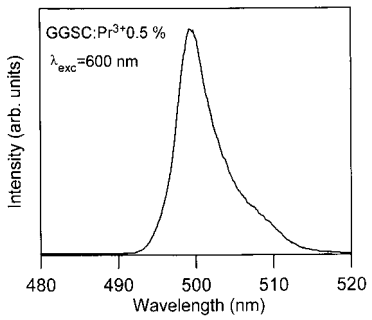

Figure 7. The fluorescence spectrum corresponding to the $^3P_0 \rightarrow {}^3H_4$ transition for GGSC glass doped with 0.5% of Pr^{3+} obtained at 77 K under excitation at 600 nm.

This upconversion process can occur via two distinct mechanisms: radiatively by an excited-state absorption or nonradiatively by an energy-transfer upconversion [25, 26]. In the first mechanism a single ion is involved, whereas two ions are involved in the second

one. As two laser photons are involved in each of the above-mentioned processes, the $^3P_0$ fluorescence shows a quadratic dependence on pump laser energy as has been observed in various systems [11–20]. Lifetime measurements provide an invaluable tool for discerning which is the operative mechanism. The radiative ESA process occurs within the excitation pulse width, leading to an immediate decay of the upconversion luminescence after excitation. Upconversion by energy transfer leads to a decay curve for the anti-Stokes emission which shows a rise time after the laser pulse, followed by a decay and a lifetime longer than that of the level $^3P_0$ under direct excitation. These effects become more pronounced as the $^1D_2$ lifetime increases [11]. This distinction only arises when the pulse width is much shorter than the time constant of the relevant energy-transfer step [32].

The time evolution of the upconverted emission from the $^3P_0$ level obtained after excitation in the $^1D_2$ state shows the latter behaviour. Figure 8 shows the decays of $^3P_0$ emission after excitation into the $^1D_2$ level for the GGSB glass with different Pr^{3+} concentrations at 77 K. The decay curves of the anti-Stokes $^3P_0 \rightarrow {}^3H_4$ emission show a certain delay (or rise) time which decreases as the Pr^{3+} concentration increases and a lifetime longer than that of the level $^3P_0$ under direct excitation. As the concentration increases the interionic distance decreases

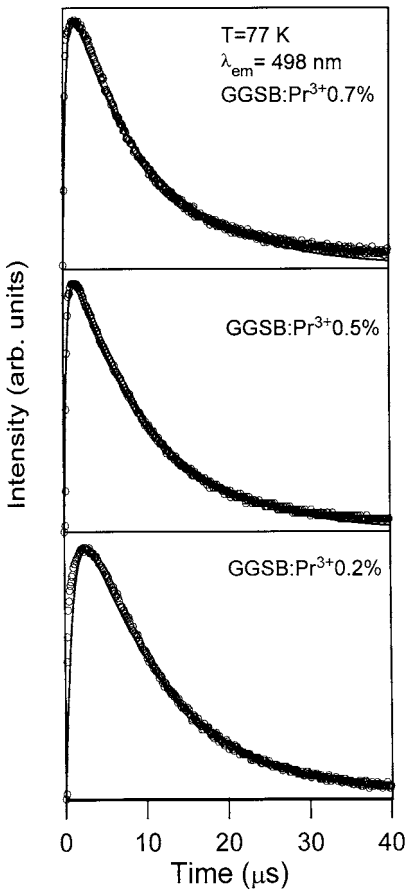

Figure 8. Experimental emission decay curves of the level $^3P_0$ obtained under excitation at 600 nm for GGSB glass doped with three different Pr^{3+} concentrations. The data correspond to 77 K. Symbols stand for the experimental data and solid lines correspond to a fit with equation (8).

and hence the energy-transfer probability increases. Therefore the rise time decreases with concentration since the transfer rate is the inverse of time. It must also be noted that the delay time depends on the lifetimes of the levels involved in the energy-transfer process. The observed rise time of the $^3P_0$ decays obtained under pulsed excitation in the $^1D_2$ state indicates that the energy-transfer process seems to be mainly responsible for the anti-Stokes fluorescence of Pr^{3+} in these glasses, though other possible mechanisms cannot be disregarded. Similar results are obtained for the three compositions. An analogous behaviour has also been observed in borate [12], fluoroindate [13], fluorophosphate [19], and germanate [20] glasses and has been attributed to a redistribution of energy between two ions according to $^1D_2 + {}^1D_2 = {}^1G_4 + {}^3P_0 + \text{phonons}$ [33]. In this model, proposed by Buisson and Vial to explain the ETU [33], when two Pr^{3+} ions are excited to the $^1D_2$ state a transfer occurs by which one ion loses energy and goes to the lower excited level $^1G_4$, while the other one gains energy and goes to the $^3P_2$ level from where, by nonradiative decay, the $^3P_0$ level is populated. The temporal behaviour of the fluorescence can be derived from rate equations for the population density of the $^1D_2$ and $^3P_0$ states. Solving the population equations, the time evolution of the $^3P_0$ emission after $^1D_2$ excitation is given by

$$I(t) = k(e^{-t/\tau_d} - e^{-t/\tau_r}) \tag{8}$$

where k is a constant, τ_d is the decay time, and τ_r is the rise time. In this model, τ_r is governed by the decay time of the $^3P_0$ state, whereas τ_d should be determined by the decay time of the $^1D_2$ level and the energy-transfer rate.

Figure 8 shows, as an example, the fitting to expression (8) for GGSB glass. Table 1 shows the rise and decay times for the three samples doped with 0.5 mol% of Pr^{3+} together with the decay times obtained under OP excitation in the level $^3P_2$. As can be seen in table 1, for all samples studied the observed rise times are much shorter than those which are predicted by this model [33]. This situation has also been found in other glasses [20] and crystals [14, 18, 34] and attributed to the limitations of the model assumed, i.e. in the concentrated Pr^{3+} systems, $^1D_2$ decay is not exponential and $^3P_0$ decay times could be different for the specific ion pairs [34]. In these chalcohalide glasses the rise time observed in the $^3P_0$ decays supports the argument that ETU is responsible for the upconversion process, though some other processes feeding the level $^3P_0$ could also occur.

Table 1. Rise and decay times (μs) of the $^3P_0$ level obtained under excitation in the $^1D_2$ level (600 nm) for the three glasses doped with 0.5 mol% of Pr^{3+} at 77 K. Lifetimes (μs) of the $^3P_0$ level obtained under direct excitation (454 nm) are also included.

	$\lambda_{exc} = 600$ nm		$\lambda_{exc} = 454$ nm
Glass; $x = 0.5\%$	τ_r (μs)	τ_d (μs)	τ (μs)
GGSC	0.2	8.3	7.8
GGSB	0.4	9.9	6.7
GGSI	0.5	12.6	6.3

4. Conclusions

(i) IR-to-orange and IR-to-blue upconversion in Pr^{3+}-doped chalcohalide glasses has been investigated under continuous-wave laser excitation for different halide modifiers. The analysis of the experimental results shows the existence of two different upconversion mechanisms (ESA and ETU) for populating both $^3P_0$ and $^1D_2$ states.

(ii) A theoretical model which takes into account the ion–phonon interaction has been developed to account for the temperature dependence of the excitation-upconverted IR-to-blue band, and gives a good explanation of the experimental results.

(iii) Orange-to-blue upconversion has also been observed in all the samples under pulsed excitation. The observed rise time of the $^3P_0$ decays obtained under pulsed excitation in the $^1D_2$ state indicates that the energy-transfer process seems to be mainly responsible for the anti-Stokes fluorescence of Pr^{3+} in these glasses, though other possible mechanisms cannot be disregarded

Acknowledgments

This work was supported by the Spanish Ministerio de Ciencia y Tecnología MCYT (reference MAT2000-1135, Acción Integrada HF99-43, and Programme SGPDE).

References

[1] Isshiki K, Kubota M, Kuze Y, Yamaguchi S, Watanabe H and Kasahara K 1998 *IEEE Photonic Technol. Lett.* **10** 1112
[2] Tawarayama H 1998 *Properties, Processing and Applications of Glass and Rare-earth Doped Glasses for Optical Fibres* vol 22 (London: INSPEC) p 355
[3] Hewak D W *et al* 1993 *Electron. Lett.* **29** 237
[4] Brady D J 1998 *Properties, Processing and Applications of Glass and Rare-earth Doped Glasses for Optical Fibres* vol 22 (London: INSPEC) p 283
[5] Guimond Y, Adam J L, Jurdyc A M, Mugnier J, Jacquier B and Zhang X H 1999 *Opt. Mater.* **12** 467
[6] Griscom L S, Adam J L and Binnemans K 1998 *J. Non-Cryst. Solids* **256+257** 383
[7] Kaminskii A A 1991 *Ann. Phys., Paris* **16** 639
[8] Allain J Y, Monerie M and Poignant H 1991 *Electron. Lett.* **27** 1156
[9] Smart R G, Hanna D C, Tropper A C, Davey S T, Carter S F and Szebesta D 1991 *Electron. Lett.* **27** 1307
[10] Auzel F 1990 *J. Lumin.* **45** 341
[11] Malta O L, Antic-Fidancev E, Lemaitre-Blaise M, Dexpert-Ghys J and Piriou B 1986 *Chem. Phys. Lett.* **129** 557
[12] Pacheco E M and Araujo C B 1988 *Chem. Phys. Lett.* **148** 334
[13] De Araujo L E E, Gomes A S L, De Araujo C B, Messaddeq Y, Florez A and Aegerter M A 1994 *Phys. Rev.* B **50** 16 219
[14] Malinowski M, Garapon C, Joubert M F and Jacquier B 1995 *J. Phys.: Condens. Matter* **7** 199
[15] Capobianco J A, Raspa N, Monteil A and Malinowski M 1993 *J. Phys.: Condens. Matter* **5** 6083
[16] Zalucha D J, Wright J C and Fong F K 1973 *J. Chem. Phys.* **59** 997
[17] Ganem J, Dennis W M and Yen W M 1992 *J. Lumin.* **54** 79
[18] Balda R, Fernández J, Sáez de Ocáriz I, Voda M, García A J and Khaidukov N 1999 *Phys. Rev.* B **59** 9972
[19] Balda R, Fernández J, Adam J L, Mendioroz A and Arriandiaga M A 1999 *J. Non-Cryst. Solids* **256+257** 299
[20] Balda R, Fernández J, de Pablos A and Fdez-Navarro J M 1999 *J. Phys.: Condens. Matter* **11** 7411
[21] Malinowski M, Joubert M F and Jacquier B 1994 *Phys. Rev.* B **50** 12 367
[22] Remillieux A and Jacquier B 1996 *J. Lumin.* **68** 279
[23] Malinowski M, Joubert M F and Jacquier B 1994 *J. Lumin.* **60+61** 179
[24] Balda R, Mendioroz, A, Fernández J, Arriandiaga M A, Griscom L S and Adam J L 2001 *Opt. Mater.* **16** 249
[25] Auzel F 1973 *Proc. IEEE* **61** 758
[26] Wright J C 1976 *Top. Appl. Phys.* **15** 239
[27] Di Bartolo B 1968 *Optical Interactions in Solids* (New York: Wiley)
[28] Henderson B and Imbusch G F 1989 *Optical Spectroscopy of Inorganic Solids* (New York: Clarendon)
[29] Fernández J, Mendioroz A, García A J, Balda R and Adam J L 2000 *Phys. Rev.* B **62** 3213
[30] Adam J L, Guimond Y, Jurdyc A M, Griscom L, Mugnier J and Jacquier B 1998 *Proc. SPIE* **3280** 31
[31] Tveryanovich A, Tveryanovich Yu S and Loheider S 1996 *J. Non-Cryst. Solids* **208** 49
[32] Wermuth M, Riedener T and Güdel H U 1988 *Phys. Rev.* B **57** 4369
[33] Buisson B and Vial J C 1981 *J. Physique Lett.* **42** L115
[34] Vial J C, Buisson R, Madeore F and Poirier M 1979 *J. Physique* **40** 913